



# **COMPUTATIONAL FLUID DYNAMICS INVESTIGATION OF PERFORMANCE OF VOLUMETRIC RECEIVERS IN SOLAR TOWER POWER PLANTS**

**By**

**Mohamed Ahmed El-Sayed Emara**

A Thesis Submitted to the  
Faculty of Engineering at Cairo University  
in Partial Fulfilment of the  
Requirements for the Degree of  
**MASTER OF SCIENCE**  
**in**  
**MECHANICAL POWER ENGINEERING**

**FACULTY OF ENGINEERING, CAIRO UNIVERSITY  
GIZA, EGYPT  
2017**

**COMPUTATIONAL FLUID DYNAMICS INVESTIGATION  
OF PERFORMANCE OF VOLUMETRIC RECEIVERS IN  
SOLAR TOWER POWER PLANTS**

**By**

**Mohamed Ahmed El-Sayed Emara**

A Thesis Submitted to the  
Faculty of Engineering at Cairo University  
in Partial Fulfilment of the  
Requirements for the Degree of  
**MASTER OF SCIENCE**  
**in**  
**MECHANICAL POWER ENGINEERING**

**Under the Supervision of**

**Prof. Dr. Adel Khalil Hassan Khalil**  
Professor  
Mechanical Power Engineering Department  
Faculty of Engineering, Cairo University

**Dr. Taher Mohamed Abou-Deif**  
Lecturer  
Mechanical Power Engineering Department  
Faculty of Engineering, Cairo University

**FACULTY OF ENGINEERING, CAIRO UNIVERSITY  
GIZA, EGYPT  
2017**

# **COMPUTATIONAL FLUID DYNAMICS INVESTIGATION OF PERFORMANCE OF VOLUMETRIC RECEIVERS IN SOLAR TOWER POWER PLANTS**

**By**

**Mohamed Ahmed El-Sayed Emara**

A Thesis Submitted to the  
Faculty of Engineering at Cairo University  
in Partial Fulfilment of the  
Requirements for the Degree of  
**MASTER OF SCIENCE**  
**in**  
**MECHANICAL POWER ENGINEERING**

**Approved by the Examining Committee**

**Prof. Dr. Adel Khalil Hassan Khalil**

**Thesis Main Advisor**

Professor, Mechanical Power Engineering Department, Faculty of Engineering, Cairo University

**Prof. Dr. Ahmed Seif Allah El Asfoury**

**Internal Examiner**

Professor, Mechanical Power Engineering Department, Faculty of Engineering, Cairo University

**Prof. Dr. Mohamed Fatouh Ahmed Mohamed**

**External Examiner**

Professor, Mechanical Power Engineering Department, Faculty of Engineering – El Mattaria, Helwan University

**FACULTY OF ENGINEERING, CAIRO UNIVERSITY  
GIZA, EGYPT  
2017**

**Engineer:** Mohamed Ahmed El Sayed Emara  
**Date of Birth :** 23/07/ 1990  
**Nationality :** Egyptian  
**E-mail :** m.a.emara@live.com  
**Phone. :** 01221905085  
**Address :** 27<sup>th</sup> M.Nussoh St., Faisal – Haram, Giza  
**Registration Date :** 1 / 10 /2014  
**Awarding Date :** / / 2017  
**Degree :** Master of Science  
**Department :** Mechanical Power Engineering



**Supervisors :** Prof. Dr. Adel Khalil Hassan Khalil  
Dr. Taher Mohamed Abou-Deif

**Examiners :** Prof. Dr. Adel Khalil Hassan Khalil  
Prof. Dr. Ahmed Seif Allah El Asfoury  
Prof. Dr. Mohamed Fatouh Ahmed Mohamed

**Title of Thesis :** Computational Fluid Dynamics Investigation of Performance of Volumetric Receivers in Solar Tower Plants

**Key Words:** CFD; Heat Transfer; Porous; Solar; Solar Receivers

### **Summary :**

In the current study, a computational fluid dynamics model was developed using volume averaged Navier-Stokes equations and porous thermal equilibrium model to investigate the performance of the solar volumetric receiver against the change of a set of parameters such as: main air inlet velocity, return air temperature, return air velocity and return air inlet orientation. The model was validated against previous experimental results with maximum outlet temperature deviation of 7.3%. A new geometry influenced by the HiTRec receiver design was proposed in order to take into account the effect of return air on receiver's performance, also to modify the outlet zone of the receiver in order to minimize flow separation and reversed flow.

The current study concluded that plants installed at locations of high wind speeds will result in poor performance of the volumetric receiver, and also showed that the thermal efficiency decreased by 14% when the inlet velocity increased from 0.2 to 1.2 m/s, moreover, using high porosity absorbers is not necessarily an advantage due to the high thermal gradients that lead to high thermal stresses, the possibility of occurrence of flow instability and distortion or failure of the absorber.

## **Disclaimer**

I hereby declare that this thesis is my own original work and that no part of it has been submitted for a degree qualification at any other university or institute.

I further declare that I have appropriately acknowledged all sources used and have cited them in the references section.

Name: Mohamed Ahmed El Sayed Emara

Date: 30/7/2017

Signature:

## **ACKNOWLEDGMENTS**

I would like to express my gratitude to my supervisors Prof. Dr. Adel Khalil and Dr. Taher Mohamed for their guidance and constant encouragement and support.

I also would like to thank Eng. Mohamed Mortada for his unconditional support and help, and my friend Eng. Mohamed Abdelazim for the fruitful debates and his unceasing assistance.

Finally, I owe a lifelong debt to my mother and father for their motivation through finishing this thesis, their patience, and care and for maintaining a perfect environment for study and research.

# Table of Contents

Disclaimer .....	ii
Acknowledgments.....	iii
Table of Contents .....	iv
List of figures .....	vi
List of Tables .....	vi
Nomenclatures .....	ix
Abbreviations.....	ix
Abstract .....	x
<b>1 CHAPTER 1: INTRODUCTION .....</b>	<b>1</b>
1.1 Solar Tower Systems.....	3
1.2 Porous Media.....	6
<b>2 CHAPTER 2: LITERATURE REVIEW .....</b>	<b>10</b>
2.1 Flow Stability .....	12
2.2 Experimental investigation.....	14
2.2.1 Wire based receivers .....	14
2.2.2 Ceramic based receivers .....	14
2.2.3 High Temperature Receiver HiTRec .....	16
2.3 Analytical investigation.....	20
2.3.1 Computational fluid dynamics .....	20
2.3.2 Permeability Coefficients.....	33
2.4 Knowledge Gap and Study Objectives.....	36
<b>3 CHAPTER 3 : MATHEMATICAL MODEL.....</b>	<b>37</b>
3.1 Fluid Dynamics .....	37
3.1.1 Continuity equation:.....	37
3.1.2 Momentum equation: .....	37
3.1.3 Energy equation: .....	37
3.2 Turbulence Modelling .....	37
3.3 Treatment of Turbulence in Porous Media in FLUENT .....	39
3.4 Receiver Thermal Efficiency .....	40
3.5 Incident Solar Heat Flux .....	40
<b>4 CHAPTER 4 : Results and Discussion .....</b>	<b>42</b>
4.1 Geometry and mesh.....	42
4.1.1 Receiver geometry .....	42

4.1.2	Mesh independence.....	43
4.1.3	Boundary cells .....	43
4.2	Operating conditions and physical properties .....	44
4.3	Validation .....	45
4.4	Parameters Matrix .....	47
4.5	Results .....	47
4.5.1	Effect of inlet velocity variation .....	47
4.5.2	Effect of return air velocity variation.....	56
4.5.3	Effect of return air temperature variation .....	58
4.5.4	Effect of return air inlet orientation variation .....	64
<b>5</b>	<b>CHAPTER 5 : Conclusions and Recommendations.....</b>	<b>68</b>
5.1	Conclusions .....	68
5.2	Recommendations for future work:.....	70
<b>6</b>	<b>References.....</b>	<b>71</b>
	<b>Appendix I – Fluent User Defined Functions .....</b>	<b>73</b>
6.1	C++ code used for defining heat flux distribution for different absorber porosities:73	
6.2	C++ code used to define thermophysical properties .....	75



## LIST OF TABLES

Table 1	Typical data of solar tower based power plants from Romero et al. (2002) cited by Avila-Marín (2011) [9]	4
Table 2	Development of volumetric receivers in the past three decades [9]	11
Table 3	Heat transfer correlations listed by Xu et al. [12]	21
Table 4	Mesh independence study summary	43
Table 5	Operating and physical conditions for the model	45
Table 6	Parameters matrix	47
Table 7	Receiver's maximum temperature and average outlet temperature for different porosities	47

## LIST OF FIGURES

Figure 1 - Carbon dioxide emission in gigaton since the industrial revolution [1].....	1
Figure 2 - IEA world fuel share [2].....	2
Figure 3 - PS10 solar power tower .....	3
Figure 4 – Rankine cycle with solar tower and thermal storage. ....	3
Figure 5 - Effect of irradiance penetration in volumetric receivers versus tube receivers [7]	5
.....	5
Figure 6 - PS10, the world's first commercial concentrating solar power tower .....	5
Figure 7 - The PS20 solar power plant near Seville in Andalusia .....	6
Figure 8 - The Ivanpah Solar Electric Generating System in California .....	6
Figure 9 – (a) Example of ceramic foam [22] (b) Examples of porous media found in nature	7
[8].....	7
Figure 10- Representative elementary volume [8].....	8
Figure 11 - Quadratic pressure difference against absorber outlet temperature at different	
values of solar flux at $K2 = \infty$ [9].....	12
Figure 12 - Quadratic pressure difference against several $K2$ values at the same solar flux	
[9].....	13
Figure 13 - The modules of the Ceramtec receiver after installation on the test bed [13].	15
Figure 14 - Assembly of the Sandia central receiver [13] .....	15
Figure 15 - The HiTRec receiver main components [13] .....	16
Figure 16 - HiTRec receiver cross section [15] .....	17
Figure 17 - Cracked HiTRec-II module [14] .....	18
Figure 18 – Interpolated flux distribution on the HiTRec-II aperture indicating the two	
cracked modules C16 and C21 (flux dimensions in $kW/m^2$ ) [14].....	18
Figure 19 - The SOLAIR 3000 receiver [6].....	19
Figure 20 - Solid and fluid phases temperature distribution for different particle diameter	
$dp$ along the absorber axis [12] .....	22
Figure 21 – Solid and fluid phases dimensionless temperature distribution $\theta$ for different	
particle diameter $dp$ along the dimensionless axis [12] .....	23
Figure 22 - Solid and fluid phases dimensionless temperature distribution $\theta$ for different	
porosity along the dimensionless axis [12].....	23
Figure 23 - Solid and fluid phases dimensionless temperature distribution $\theta$ for different	
absorber thicknesses $L$ along the dimensionless axis [12].....	24
Figure 24 - Solid and fluid phases dimensionless temperature distribution $\theta$ for different	
inlet velocities $u_0$ along the dimensionless axis [12] .....	24
Figure 25 – Proposed geometry by Wu et al. [11] .....	25
Figure 26 - Computational domain used by Wu et al. [17].....	25
Figure 27 – Static pressure drop profile across the absorber [17].....	26
Figure 28 – Mean velocity fluctuations across the absorber [17] .....	27
Figure 29 – Dimensionless temperature profile across the absorber [17].....	27
Figure 30 - Wu et al. (2011) validation curve [17] .....	28
Figure 31- Different porosity arrangement used by Roldan et al. (2014) [18] .....	29
Figure 32- Temperature contours for the fixed porosity absorbers: (a) porosity = 0.48, (b)	
porosity = 0.64, (c) porosity = 0.78 [18].....	31
Figure 33 - 2D geometry for the Roldan's model [15].....	32
Figure 34 – Mesh and main boundary conditions for Roldan's model [15].....	32
Figure 35 – Validation chart for the four cups in Roldan's model [15] .....	33
Figure 36 - Deviations of granular media correlations from experimental pressure drop	
across ceramic foam [19].....	34

Figure 37 – 3D geometry used by Wu et al. (2010) [17] .....	35
Figure 38 - Pressure drop versus velocity comparison between Wu's correlation (Correlation 10 in the plot) and other models [20] .....	36
Figure 39 – Measurements of velocity fluctuations in a turbulent flow [22].....	38
Figure 40 – Thermal camera absorber image [18] .....	40
Figure 41 – Theoretical and actual absorber temperature distribution [18].....	41
Figure 42 - Proposed geometry .....	42
Figure 43 – Model mesh .....	43
Figure 44 - Boundary cells inflation .....	44
Figure 45 - Validation curve between current study, Roldan et al. (2014) and experimental work [18].....	46
Figure 46 - Receiver outlet temperature distribution for porosity = 0.48 at different inlet velocities .....	48
Figure 47 - Receiver outlet temperature distribution for porosity = 0.64 at different inlet velocities .....	49
Figure 48 - Receiver outlet temperature distribution for porosity = 0.78 at different inlet velocities .....	50
Figure 49 - Absorber temperature difference versus inlet velocity at constant return air of 390 K, for the 0.48 porosity absorber .....	51
Figure 50 - Absorber temperature difference versus inlet velocity at constant return air of 390 K, for the 0.64 porosity absorber .....	52
Figure 51 - Absorber temperature difference versus inlet velocity at constant return air of 390 K, for the 0.78 porosity absorber .....	53
Figure 52 - Average outlet temperature versus inlet velocity .....	54
Figure 53 - Thermal efficiency of the receiver versus inlet velocity .....	55
Figure 54 - Receiver temperature contours at different velocities for porosity = 0.78 .....	56
Figure 55 - Return air velocity versus receiver thermal efficiency (at 500 K return air) .....	57
Figure 56 - Return air velocity versus outlet temperature (at 500 K return air) .....	58
Figure 57 – Receiver thermal efficiency versus return air temperature.....	59
Figure 58 – Receiver average outlet temperature versus return air temperature .....	60
Figure 59 – Receiver temperature contour for the 0.78 porosity absorber at return temperature of 390 K .....	61
Figure 60 – Receiver temperature contour for the 0.78 porosity absorber at return temperature of 500 K .....	62
Figure 61 – Receiver temperature contour for the 0.78 porosity absorber at return temperature of 600 K .....	63
Figure 62 – Receiver temperature contour for the 0.78 porosity absorber at return temperature of 700 K .....	64
Figure 63 - Absorber temperature distribution at inlet velocity = 1 m/s and porosity = 0.48 for different inlet orientations. ....	65
Figure 64 - Absorber temperature distribution at inlet velocity = 1.5 m/s and porosity = 0.48 for different inlet orientations. ....	66
Figure 65 - Horizontal and vertical inlet temperature contours for the three porosity absorbers .....	67

## NOMENCLATURES

### *Variables*

$d_p$	Average pore diameter (m)
$g$	Gravitational acceleration, m/s <sup>2</sup>
$F_{Peak}$	Irradiance peak, W/ m <sup>2</sup>
$h$	Heat transfer coefficient (W/ m <sup>2</sup> .k)
$I$	Intensity of the solar radiation (W/ m <sup>2</sup> )
$I_0$	Initial intensity of the solar radiation (W/ m <sup>2</sup> )
$I_{s0}$	Superficial heat source (W/ m <sup>2</sup> )
$J$	Diffusion flux, kg/s m <sup>2</sup>
$K_1$	Viscous permeability coefficient (m <sup>2</sup> )
$K_2$	Inertial permeability coefficient (m)
$\dot{m}$	Mass flow rate (kg/sec)
$Nu$	Nusselt number
$P$	Pressure (Pa)
$q_{rec}$	Actual heat input to the receiver.
$Re$	Reynolds number
$V$	Velocity vector (m/s)
$x, y, z$	Cartesian coordinates (m)

### *Greek letters*

$\alpha$	Specific area (m <sup>-1</sup> )
$\varepsilon$	Porosity
$\mu$	Dynamic viscosity (kg/m.s)
$\rho$	Density (kg/m <sup>3</sup> )
$\zeta$	Optical extinction coefficient (m <sup>-1</sup> )
$\tau$	Shear stress tensor (N/m <sup>2</sup> )
$\eta$	Thermal efficiency

### *Subscripts*

eff	Effective
$f$	Fluid
$s$	Solid
tot	Total
$v$	Volume

## Abbreviations

CFD	Computational Fluid Dynamics
CSP	Concentrated Solar Power
DLR	Deutsches Zentrum für Luft- und Raumfahrt (German Aerospace centre)
HiTRec	High Temperature Receiver
IEA	International Energy Agency
PSA	Plataforma Solar de Almeria

## ABSTRACT

In the current study, a computational fluid dynamics model was developed using volume averaged Navier-Stokes equations and porous thermal equilibrium model to investigate the performance of the solar volumetric receiver against the change of a set of parameters. The model was validated against experimental results with maximum outlet temperature deviation of 7.3%.

A new geometry influenced by the HiTRec receiver design was proposed in order to take into account the effect of return air on receiver performance, also to modify the outlet zone of the receiver in order to minimize flow separation and reversed flow and to allow modular cup design.

A total number of 21192 cells was used for the 2D mesh and a maximum  $y^+$  value of 3.5 at the first boundary cell, and the k-epsilon turbulence model with standard wall treatment was employed.

Moreover, a Beer-Lambert distributed solar flux was used to simulate the effect of radiation penetration inside the absorber body, 3 different porosity absorbers were studied 0.48, 0.64 and 0.78, with 3 distinct extinction coefficients for the Beer-Lambert distribution, the solar flux and thermophysical properties were added to the model through C++ user defined function.

As a summary to the goals of the current study, the return air temperature plays a significant role in modular design of volumetric solar receiver cups, as both a regenerative factor and a coolant to the absorber cup structures.

When the return air acts as a coolant, it could prevent mechanical failure of the absorber due to high thermal stresses as was shown in the earliest stages of receiver development, and thus the velocity of the return air shall be optimized in order to obtain a suitable heat transfer rate between the return air stream and the cup surface when the system is bounded to a specific return air temperature, for this reason the current study investigated a wide range of return air velocities and temperatures to find its effect on the overall thermal performance of the receiver.

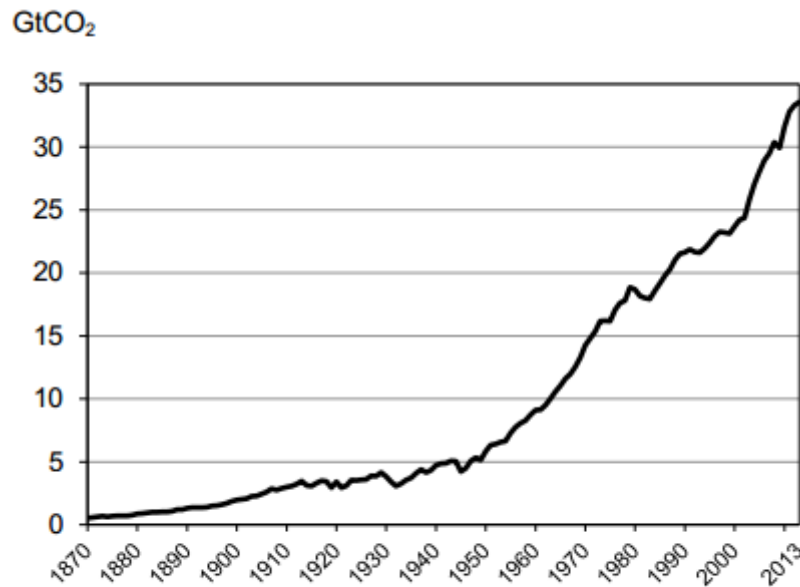
Moreover, the effect of inlet air mass flow rate was studied with the intention of investigating the different thermal profiles that could exist on the absorber body to minimize thermal gradients and thus thermal stresses, and to find its effect at the same time on the thermal efficiency and outlet temperature.

The current study found that increasing the porosity increases the thermal efficiency of the receiver and the outlet temperature, a value of 1900 K maximum temperature was obtained at the highest porosity absorber of 0.78, also a set of inlet velocities was studied to obtain absorber thermal distribution, in order to minimize thermal gradients, it was found that at inlet velocity of 1.2 m/s the temperature difference across the absorber was only 111 K.

It was also found that increasing the return air temperature while maintaining a constant return air velocity decreases the thermal efficiency of the receiver due to the reduction of the return air density. Moreover, two different return air orientations were studied in order to investigate whether the absorber temperature distribution would differ or not, however, it was found that the difference between the two cases was not significant.

# 1 INTRODUCTION

Since the industrial revolution in the 18<sup>th</sup> century, fossil fuels have accompanied mankind towards a vast scientific and technological progress. However, with the current depletion rate of fossil fuel and the environmental effects that rose from the carbon dioxide emissions, as the 2016 “*International Energy Agency (IEA) CO<sub>2</sub> emission from fuel combustion*” report stated that CO<sub>2</sub> emissions increased from around zero to higher than 32 Gigatons CO<sub>2</sub> in 2014 [1], hence, the transition to a dependence on renewable, sustainable and clean energy sources is a crucial step for a better future.



Source: Carbon Dioxide Information Analysis Center, Oak Ridge National Laboratory, US Department of Energy, Oak Ridge, Tenn., United States.

Figure 1 - Carbon dioxide emission in gigaton since the industrial revolution [1]

According to the IEA annual report (Figure 2) more than 80% of world fuel share is based on hydrocarbon fuels [2] (oil, natural gas and coal)

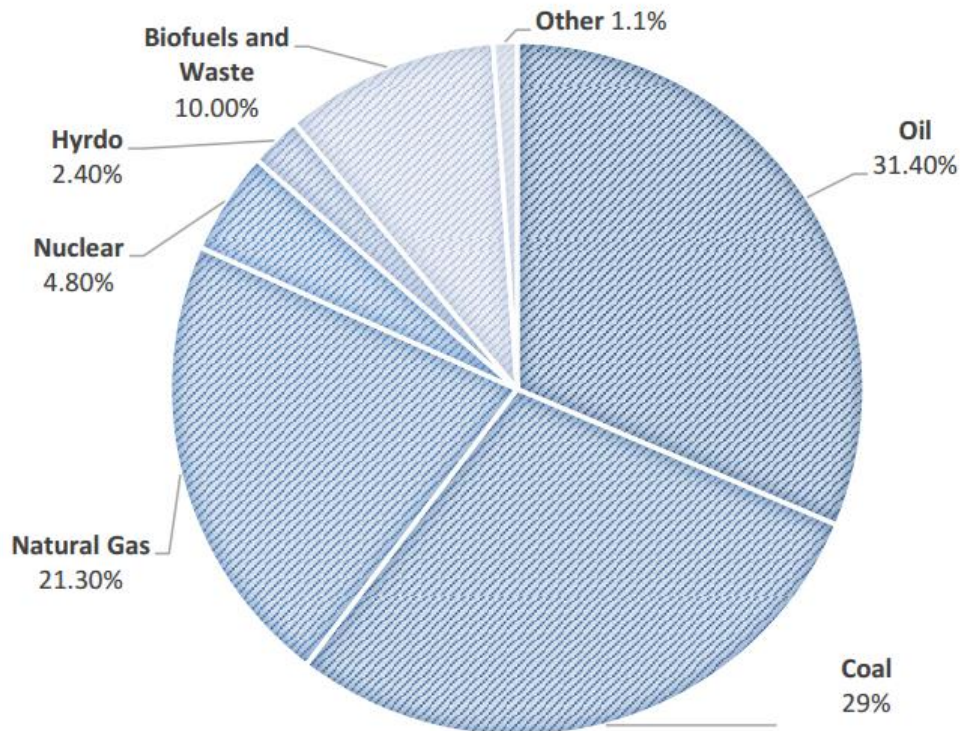


Figure 2 - IEA world fuel share [2]

Solar energy has the potential of being an adequate energy source to fulfil current world's requirements of power, being clean and permanent, Earth receives a daily solar energy of around  $6.26 \times 10^{20}$  Joules per hour [3], but due to the intermittent nature of solar power as a result of cloud movements, seasonal change and being costly when compared to conventional power plants [4], there is a great challenge for any energy system that utilizes solar energy.

Another drawback of solar energy is the low density of the irradiated flux on Earth surface, resulting in a need for concentrating solar flux for large scale power production.

One of the intensively examined solar technologies in the past three decades is concentrated solar power (CSP) systems.

An example of concentrated solar power systems is solar tower based power plants, where concentration is achieved mainly by an array of heliostat mirrors having a common focal spot (the solar tower) where the receiving system is mounted (Figure 3), the receiver then transfers the solar flux to a working fluid of a thermal power cycle (Rankine or Gas turbine for example – Figure 4).